Separation Science and Technology
Publication details, including instructions for authors and subscription information:
http://www.informaworld.com/smpp/title~content=t713708471

DESIGN METHODOLOGY FOR THE OPTIMIZATION OF MEMBRANE SEPARATION PROPERTIES FOR HYBRID VAPOR PERMEATION-DISTILLATION PROCESSES

Alaa Fahmy[a]; Dieter Mewes[a]; Katrin Ebert[b]
[a] Institut für Verfahrenstechnik, Universität Hannover, Hannover, Germany [b] Institut für Chemie, Geesthacht, Germany

To cite this Article Fahmy, Alaa , Mewes, Dieter and Ebert, Katrin(2001) 'DESIGN METHODOLOGY FOR THE OPTIMIZATION OF MEMBRANE SEPARATION PROPERTIES FOR HYBRID VAPOR PERMEATION-DISTILLATION PROCESSES', Separation Science and Technology, 36: 15, 3287 — 3304

To link to this Article: DOI: 10.1081/SS-100107903

URL: http://dx.doi.org/10.1081/SS-100107903

SEPARATION SCIENCE AND TECHNOLOGY, 36(15), 3287–3304 (2001)

DESIGN METHODOLOGY FOR THE OPTIMIZATION OF MEMBRANE SEPARATION PROPERTIES FOR HYBRID VAPOR PERMEATION-DISTILLATION PROCESSES

Alaa Fahmy,[1] Dieter Mewes,[1],* and Katrin Ebert[2]

[1]Institut für Verfahrenstechnik, Universität Hannover,
Callinstr. 36, D-30167 Hannover, Germany
[2]GKSS Forschungszentrum, Institut für Chemie,
Max-Planck-Str., D-21502 Geesthacht, Germany

ABSTRACT

Hybrid processes of distillation and vapor permeation are considered promising alternatives to azeotropic and extractive distillation. The research is directed toward developing membranes with improved separation properties and longer life times.We show that membranes with very high selectivities are not desirable when a very high purity of the retentate is required. A design methodology was developed to calculate the optimum separation properties for the membranes within hybrid processes. The results of the simulation encourage the use of low-selectivity membranes, especially if the membrane step is coupled to a distillation step. The method is applied to an ethanol dehydration process. However, it can be applied to other membrane separation processes as well.

---

*Corresponding author. Fax: +49/511/7623031; E-mail: dms@c36.uni-hannover.de

www.dekker.com

Key Words: Vapor permeation; Hybrid; Distillation; Process design; Optimization

INTRODUCTION

Hybrid processes of distillation and membrane separation processes have gained much attention in recent years. The results of this coupling benefit from the specific advantages of each separation step: the low cost of distillation and the independence of the membrane process on the boiling curve of the phase diagram. Typical implementation areas of hybrid processes are closely boiling and azeotropic separations. These hybrid processes can offer cost savings when compared to conventional azeotropic, extraction, or 2-pressure distillation processes.

Pressly and Ng (1) presented a review of the economical aspects of hybrid processes. They suggested a break-even analysis for investigating the feasibility of various types of distillation-membrane hybrids. Lipnizki, Field, and Ten (2) presented a review of process design and the economics of pervaporation-based hybrid processes. Stephan, Noble, and Koval (3), Pettersen et al. (4), and Moganti, Noble, and Koval (5) analyzed olefin purification by a distillation-membrane hybrid process. They studied different process configurations for determining the optimal operating conditions for each configuration. Their optimization analysis was restricted to the calculation of the membrane area and the number of theoretical column trays. Pettersen and Lien (6) presented parametric studies illustrating some of the trade-offs in a hybrid distillation-membrane process for ethanol dehydration. Their calculations were based on an algebraic model for describing mass transport through the membrane. Rautenbach et al. (7) optimized a hybrid process for separating methanol from dimethylcarbonate by calculating the processing cost. The feed and retentate stream composition were the variables manipulated for this membrane study.

The membrane process may be a pervaporation or a vapor permeation unit. Both processes are closely related, differing only in the state of the feed. For pervaporation, the feed is liquid and the permeate evaporates through the membrane. The heat supply to the feed stream is usually accomplished by intermediate heat exchangers that are installed between a number of pervaporation modules in series. For vapor permeation, the feed is vapor, which does not change phase while crossing the membrane surface making the process less complex. For both processes the driving force for material transport through the dense membrane is the difference in the chemical potential of the permeating components between the feed and permeate side. This driving force is usually realized through lowered pressure on the permeate side. Vapor permeation is especially suitable for the purification of top streams of fractionation columns that can be used as feed directly. Although vapor permeation is less sensitive to concentration polarization at the feed side of the membrane, the mass transport is sensitive to the degree of superheating and to friction losses in the feed side. On one hand, little superheating lowers the transmembrane flux in polymeric membranes as a result of decreased sorption and swelling. On the other hand, heat losses due to friction can result in the formation of an undesired condensate film that partially covers the membrane on the feed side. Brüschke and Schneider (8) invented a process that combines both vapor permeation and pervaporation in which the feed is introduced as a liquid-vapor mixture that flows up a vertically mounted membrane module. This process results in a complete mixing of the 2 phases, and a stationary liquid film does not form on the membrane surface. The mass transport could be improved by insuring saturation conditions throughout the feed side of the membrane. Detailed investigations on vapor permeation and its comparison to pervaporation are reported in the literature (9–17).

Various types of membranes have been investigated for pervaporation and vapor permeation (8–20). Poly(vinyl alcohol) (PVA) membranes are considered standard dehydration membranes because of their high selectivities and their relatively high fluxes in many aqueous organic solutions. Research is directed toward producing membranes of higher fluxes with reasonable selectivities. Our aim in the present work was to illustrate a design method for the determination of the optimum selectivity of the membranes required for a certain separation process. This goal was achieved through the minimization of the annual cost of the complete membrane process as a function of the membrane separation properties. The method was applied to the dehydration of ethanol in which 99.9% product purity was required.

Simulation Models

The mass transfer through the membrane is based on sorption-diffusion-desorption steps. Rigorous modeling requires the simulation of these steps. The prediction of the mixture solubilities using the UNIQUAC model, which gives very good results in the case of polar liquid mixtures and hydrophilic membranes (21), can be made. However, no promising models for the prediction of the mixture diffusivities have been found. Great effort has been directed toward modeling the mass transport through molecular modeling (22–24). Reasonable results of a detailed molecular-dynamics simulation have been illustrated, but they are unfortunately limited to the feed-polymer interface. More extensive results are still expected from this simulation methodology.

We present a general model for material balance and membrane area calculations. It is valid for binary mixtures. The main assumptions in this model are

1. negligible pressure drop along either side of the membrane surface,
2. plug flow along the feed side of the membrane, and
3. cross flow along the permeate side of the membrane.

The vapor permeation module with the main design variables is shown schematically in Fig. 1. All the mass fractions refer to the faster permeating component. A mass balance based on a differential element of the membrane results in the following equation:

$$\frac{dm^{\mathrm{F}}}{m^{\mathrm{F}}} = \frac{dx^{\mathrm{F}}}{x^{\mathrm{P}} - x^{\mathrm{F}}} \tag{1}$$

where m and x are the local mass flow rate and the local mass fraction respectively. The superscripts refer to the location at the feed (F) or permeate (P) side. The integration of Eq. (1) along the concentration interval from feed to retentate gives the ratio of permeate flow rate m_{P} to feed flow rate m_{F}.

$$\theta = \frac{m_{\mathrm{P}}}{m_{\mathrm{F}}} = 1 - \exp\left(\int_{x_{\mathrm{F}}}^{x_{\mathrm{R}}} \frac{dx^{\mathrm{F}}}{x^{\mathrm{P}} - x^{\mathrm{F}}}\right) \tag{2}$$

The ratio θ is called the "module cut rate" and introduces additional mass balance information to the overall and component mass balance equations. The subscripts F, P, and R refer to the overall feed, permeate, and retentate streams.

The change in flow rate along the feed side with respect to the membrane area is expressed by the total permeation flux J_{P}.

$$\frac{dm^{\mathrm{F}}}{dA} = J_{\mathrm{P}} \tag{3}$$

By rearranging and integrating Eq. (3), the membrane area A can be calculated. The total permeation flux J_{P} must be expressed as a function of the local mass flow at the feed side m^{F}.

$$A = -\int_{m_{\mathrm{F}}}^{m_{\mathrm{R}}} \frac{dm^{\mathrm{F}}}{J_{\mathrm{P}}(m^{\mathrm{F}})} \tag{4}$$

An approximate calculation (25) of the local transmembrane flux for each permeating component i based on the solution-diffusion model may be carried out by the

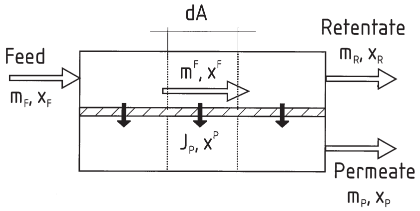

Figure 1. Schematic diagram of a vapor permeation module showing the material balance variables and flow assumptions.

equation

$$J_{\mathrm{Pi}} = \frac{S_{\mathrm{i}} D_{\mathrm{i}} \overline{\phi}_{\mathrm{i}}}{\delta f_{\mathrm{io}}} (p_{\mathrm{iF}} - p_{\mathrm{iP}}) = L_{\mathrm{i}} (p_{\mathrm{iF}} - p_{\mathrm{iP}}) \tag{5}$$

where S_{i} is the solubility coefficient of the component in the membrane polymer, and D_{i} is the diffusion coefficient of the component inside the membrane of the thickness δ. $\overline{\phi}_i$ is the average fugacity coefficient of the component at the separation conditions and can be taken as unity for low pressures. f_{io} is the standard or reference fugacity. L_{i} is the individual permeability coefficient of component i. It can be determined experimentally for each component of the mixture. The driving force is expressed in terms of the partial pressure difference of component i between the feed and permeate sides.

The selectivity of the membrane can be expressed either by the selectivity coefficient

$$\alpha_L = \frac{L_{\mathrm{a}}}{L_{\mathrm{b}}} \tag{6}$$

or by the separation factor

$$\alpha_x = \frac{x_{\mathrm{P}}/(1 - x_{\mathrm{P}})}{x_{\mathrm{F}}/(1 - x_{\mathrm{F}})} \tag{7}$$

Semi-empirical models have been suggested to relate the permeability coefficient to the process parameters (11,12). For a 2-component system, nine semi-empirical parameters must be determined experimentally.

However, at the early design stage the necessary information (experimental data) may not be available for the parameters to be determined with significant accuracy. Petersen and Lien (6) presented an algebraic model that can be used to solve the material balance around the membrane and calculate the required surface area for a specified separation through an averaged separation factor and an averaged flux of the membrane for the investigated concentration interval. This model was first published in the work of Naylor and Backer (26), who derived a calculation approach for the gaseous-diffusion-stage similar to the methods McCabe and Thiele used for distillation. The calculation procedure can be summarized in the following algebraic equations:

$$\theta = \frac{m_{\mathrm{P}}}{m_{\mathrm{F}}} = 1 - \exp\left\{\frac{1}{\overline{\alpha}_x - 1}\left[\ln\left(\frac{x_{\mathrm{R}}}{x_{\mathrm{F}}}\right) - \overline{\alpha}_x \times \ln\left(\frac{1 - x_{\mathrm{R}}}{1 - x_{\mathrm{F}}}\right)\right]\right\} \tag{8}$$

$$A = \frac{m_{\mathrm{F}}\theta}{\overline{J}_{\mathrm{P}}} \tag{9}$$

where $\overline{J}_{\mathrm{P}}$ and $\overline{\alpha}_x$ are the logarithmic mean values of the total flux and the separation factor of the membrane at the feed and retentate compositions.

In addition to the earlier stated general assumptions, this model is based on the assumption that a linear relationship exists between J_{P} and x^{F} and between ln

α_x and x^F. This assumption is valid only if the fugacity or the partial pressure of the permeate side is of a negligible value when compared to that of the feed. The flux can then be considered proportional to the concentration or partial pressure of the faster permeating component in the feed side. This is a reasonable assumption for the dehydration processes if the required purity of the retentate is not very high. A considerable amount of water will still be on the feed side, which keeps the driving force high; that is, $p_{iF} \gg p_{iP}$. An application with a relatively high driving force along the whole membrane is overcoming the azeotrope through the dehydration of isopropanol. The required separation is 85–89% isopropanol. The dehydration of ethanol, is an example in which a high product purity is desired; the subazeotropic ethanol must be concentrated from <95.5% up to 99.5% or higher. For this type and for similar dehydration problems, the local flux is not a linear function of the local feed-side composition.

When these nonlinearities appear, the algebraic model will not provide sufficient accuracy, and the design calculations must be carried out with Eqs. (1–5).

Illustrative Example

The following example demonstrates the importance of selecting a proper membrane selectivity for a separation task. The calculations are carried out with the differential model through the implementation of Eqs. (1–5). In the selected process, 1000 kg/h of an aqueous ethanol must be dehydrated from 93% (wt) up to 99.9%. For the first calculations, a PVA membrane is selected. Its water permeability is comparable to that of a Sulzer ChemTech (formerly GFT) standard dehydration membrane (10,12,13) and to the modified PVA membrane of GKSS (18). A selectivity coefficient of 2000 is assumed. Constant permeation coefficients for water and ethanol were assumed to be in line with the investigated concentration interval. This assumption could be accepted for narrow concentration intervals, especially in this early design phase, where no extensive experimental data are available for the membranes. More exact assumptions could be considered in a later phase of design and optimization in a second iteration after the suggested membranes have been developed and tested. The feed pressure was 1 bar and the permeate pressure was 20 mbar. Figure 2 represents the driving force for water transport and the required membrane area as functions of the retentate composition. The driving force is represented as the partial pressure difference between feed and permeate. A great increase of the required membrane area was observed after 99% concentration, where the driving force nearly vanished. To increase the driving force for fixed feed conditions, either the permeate pressure p_p or the permeate water concentration x_p should be lowered. Lowering the permeate water concentration can be realized through the use of a less selective membrane.

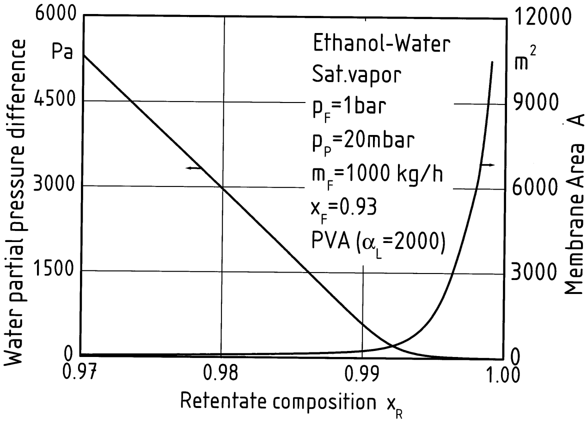

Figure 2. Difference of the water partial pressure across the membrane and the required membrane area as functions of the retentate composition.

Figure 3 shows how far the driving force could be increased in the last concentration region by the use of low selectivity membranes. Low selectivity is realized during the simulation by increasing the ethanol permeation coefficient. The water permeation coefficient is assumed to equal that of the high selectivity membranes. This assumption about permeation is very conservative because low selectivity membranes would offer a higher permeability for water. The pressure on

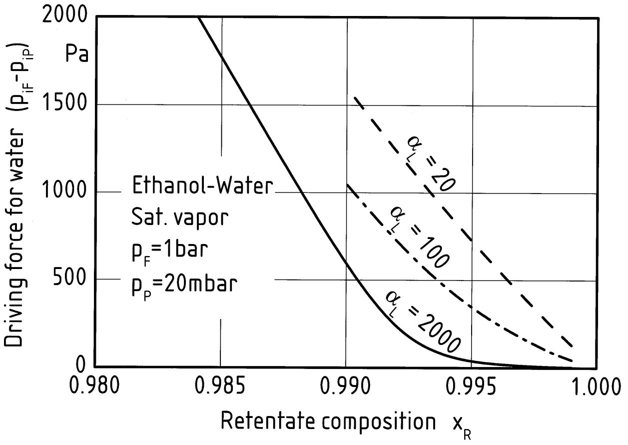

Figure 3. Driving force for water as a function of the retentate composition for different selectivity values.

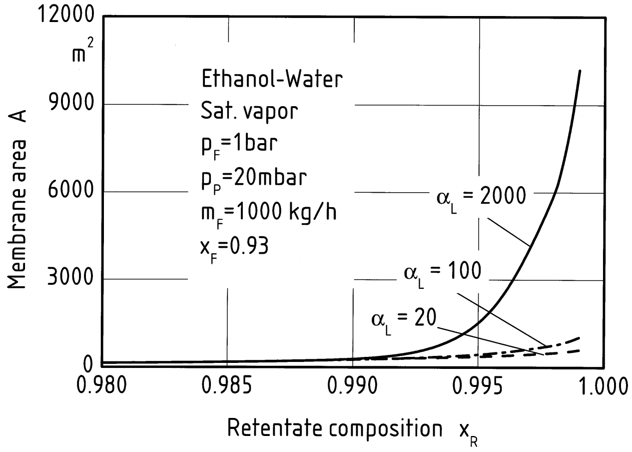

Figure 4. The required membrane area as a function of the retentate composition for different selectivity values.

the permeate side is also held constant to limit the investigation to the effect of the selectivity.

Figure 4 shows the decrease of the required membrane area achieved through the use of 2 low selectivity membranes. In these cases, the ethanol concentration in the permeate stream was higher than when high selectivity membranes were used. However, if the permeate stream were recycled to a distillation column, no ethanol would be lost. In this hybrid combination, care should be taken to ensure that ethanol is recycled back into the proper position in the column.

The increased mass flow of the permeate stream due to the presence of high levels of ethanol is shown in Fig. 5. This increase in flow rate would elevate the cost of the condensation and vacuum system of the permeate. Nevertheless, one can expect cost savings by using the membrane of $\alpha_L = 100$ because the enormous savings in the membrane area would not be abrogated by a 20% increase in the permeate flow.

The results of mass balance calculations for the hybrid process are shown in Fig. 6. The calculations are based on a column feed of 7% (wt) ethanol, which is a typical composition of the product beer of a fermentation unit (27).

These results show that the mass flow of the recycled permeate stream is always lower than 1% of the column feed, so its recycle will not result in hydrodynamic problems in the column.

Optimization Calculations

To find the optimum selectivity of the membranes for the above defined separation problem, the whole membrane system must be predesigned, the major

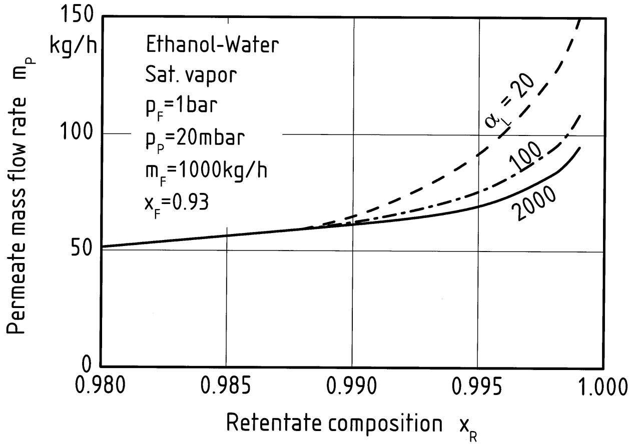

Figure 5. Permeate mass flow rates as a function of the retentate composition for different selectivity values.

equipment must be sized, and the annual cost should be minimized. For this purpose a simulation program was developed with the program ASPEN Plus. The main flow sheet and the main calculation loops are shown in Fig. 7. A developed user model allows one to calculate the material balance around the membrane, the required membrane area, and the membrane and module costs. The material balance is determined through the use of Eqs. (1–5) of the differential model previously described. A leakage air stream is inevitable in any vacuum system; however, the amount of leakage is important for subsequent calculations of the

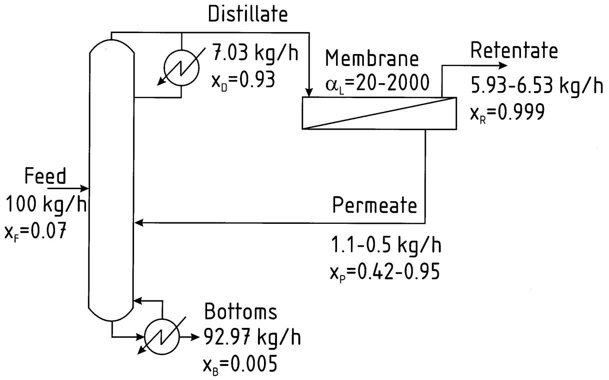

Figure 6. Mass balance for the hybrid process of ethanol dehydration. A large selectivity range is covered. All the mass fractions given are for ethanol.

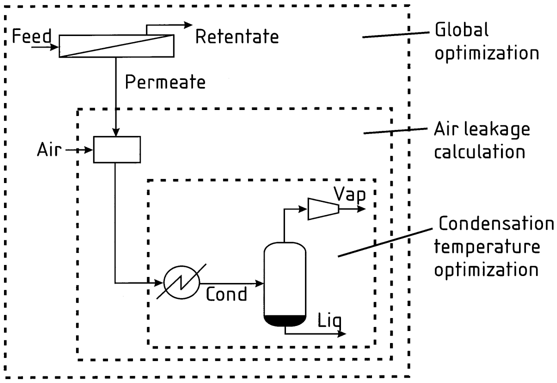

Figure 7. Main loops of the optimization program.

condenser and the vacuum pump. An air stream of assumed volume is mixed with the permeate stream and sent to the condenser. To decrease the load to the vacuum pump, the permeate mixture is condensed and subcooled. Only a very small equilibrium amount will remain with the leakage air in the gaseous phase. The condensation temperature is varied within an iteration loop. The results of creating this simulation loop were the determination of heat transfer area and the condenser volume, the design specifications of the refrigeration unit and the vacuum pump, and the total annual cost of this condensation and vacuum system. The result of using the inner loop was the determination of optimum subcooling temperature, which gives the minimum total cost of this part of the system. From the calculated condenser volume, the flow of the leakage air stream was corrected and the outer loop of the leakage air was run until it converged to a constant air stream. The global variables that could be manipulated through the whole program were membrane selectivity (i.e., the ethanol permeation coefficient) and the permeate pressure. The water permeation coefficient was held equal to that of the most selective membrane.

A typical structure of the total annual cost calculation is presented in Fig. 8. The membrane replacement costs held the highest share of the total annual cost because of the increased specific area of the membrane required as the required purity is exceedingly high. Throughout these cost calculations, the membrane material is depreciated within two years, and all the other parts of the system within five years. The cost of the membrane material was assumed to be 150 DM/m^2, while the fixed cost of the membrane modules was taken as 500 DM/m^2 of the membrane area (28). Other cost functions developed for the fixed and operating costs, as noted from several manufacturer offers, were regressed. Electric power costs are the main operating costs of the refrigeration system and of the vacuum pump. The total cost

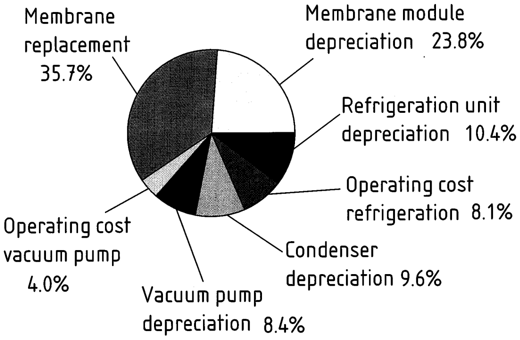

Figure 8. Typical annual cost structure of the membrane unit: $m_F = 1000$ kg/h; $x_F = 0.93$; $x_R = 0.999$; $p_F = 1$ bar; $p_p = 8$ mbar; $\alpha_L = 40$.

as the sum of the mentioned costs in Fig. 8 is illustrated in Fig. 9 as the function of the manipulated variables, the selectivity, and permeate pressures. Some of the curves are broken. If they had not been broken the data would show that the temperature of the heat transfer surface in the condenser was lower than the freezing point of the permeate mixture. This could result in the formation of ice crystals on the heat transfer surface, which could block the operation. The curves show optimum selectivities between 20 and 40 and optimum operating pressures between 4 and 6 mbar. These low selectivities may be a surprising result; however this result is specific for this separation problem in which a very high purity was required.

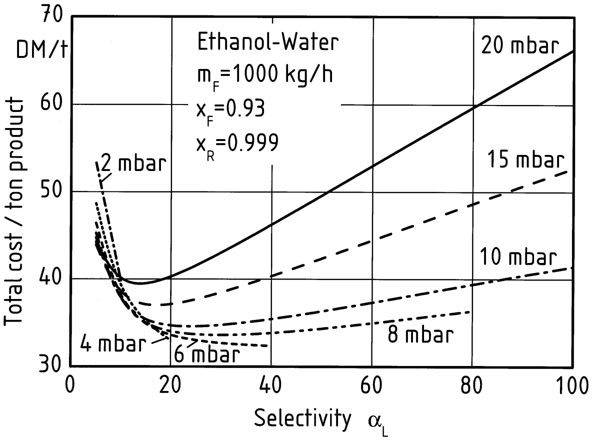

Figure 9. The membrane unit total cost as function of the membrane selectivity and the permeate pressure.

MARCEL DEKKER, INC.
270 Madison Avenue, New York, New York 10016

Table 1. Optimization Results for Three Different Process Schemes

		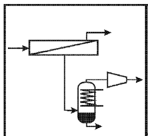	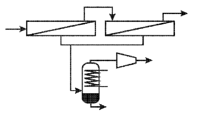		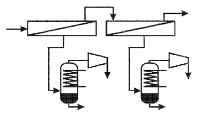	
			1st mem.	2nd mem.	1st mem.	2nd mem.
93%–99.9%	p_p	6 mbar	6 mbar		10 mbar	4 mbar
	α_L	30	100	20	40	20
	rel. cost.	100	94.3		96.2	
83%–99.9%	p_p	8 mbar	8 mbar		10 mbar	4 mbar
	α_L	40	200	20	1000	40
	rel. cost.	100	89.7		85.9	

The same methodology was used to compare three different process schemes, which are shown in Table 1. The first is a conventional scheme with one type of membrane equipped with a condensation and vacuum system. The second utilizes two different types of membranes in series integrated in the same system. In the third scheme the two membranes have different condensation and vacuum systems. The three schemes were studied for two different separation tasks, one is to increase dehydration from 93.0 to 99.9%, and the other is to increase it from 83.0 to 99.9%. The composition between the two membranes is assumed to be 99% (wt) ethanol for the last two cases. The results are shown in Table 1. A heuristic rule was derived: A higher selective membrane is needed at high concentrations of the faster permeating component, and a lower selectivity is favored for the regions of lower concentration. Based on the assumption of constant water permeability, the use of two different membranes in series will bring savings of up to 6% of the total annual cost for the first separation and up to 14% in the second separation in which the concentration interval is larger.

DISCUSSION

The general assumptions of negligible pressure drop, constant temperature, plug flow along the feed side, and cross flow along the permeate side are discussed in detail in the paper of Pettersen and Lien (6) and of Naylor and Backer (26). The assumption that the less selective membranes have the same water permeation coefficient as the most selective membranes is a very conservative assumption concerning the calculation of the membrane area and the membrane cost. Usually the less selective membranes allow higher fluxes (9). Therefore, the cost savings of the less selective membranes demonstrated in the separation example were considered to be safe calculations. Much more cost savings would be expected if the increase of the water flux as a result of a decreased selectivity were a part of the calculation.

For separations through which the water concentration in the retentate is relatively high, such as when the azeotrope of the isopropanol water system is broken, the low selectivity membranes would not appear to provide any cost savings if the calculations were carried out on the basis of the previously mentioned assumption of constant flux. However, if the flux increases observed when the selectivity is lowered were integrated in the calculations, use of low selectivity membrane would show cost savings.

The solid curve of Fig. 10 may represent the real behavior of the flux against selectivity of different membranes with different selectivities for the same separation application. During the analysis, the horizontal dotted line was assumed as the flux was held constant despite lowered selectivity of the membrane. As a first approximation, one could assume an inverse proportionality between flux and selectivity as shown by the straight dashed line of the same figure. These assumptions allow for the optimization calculations to be carried out for membranes of the same separation index as defined by $SI = J \times \alpha$. This calculation is analogous to the concept of the pervaporation separation index introduced by Huang (29).[1] The most exact relation between the flux and the selectivity of the considered

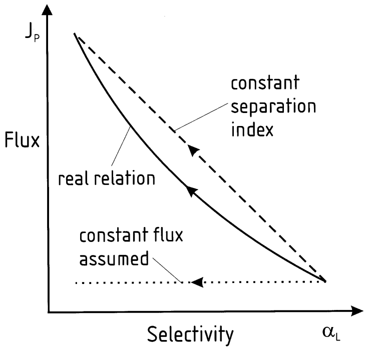

Figure 10. Relationship between flux and selectivity shown schematically for 1 membrane type.

---

[1] Another common separation index is the Rony's extent of separation (30), which was refined by Sirkar (31) for single entry barrier separation processes. This index has been extensively used for the characterization of gas separation stages (32,33) and pervaporation (34).

membranes should be derived experimentally. Therefore, a number of different membranes with different separation properties must be developed for the same application. These membranes must be tested experimentally for one to get an idea about flux variation with respect to selectivity for the membrane. Moreover, relationships between the permeation coefficient and the process parameters should be determined for each membrane. This determination requires that a targeted set of experiments be completed to increase the accuracy of the optimization procedure. Nevertheless, though our optimization may not give the most accurate quantitative result, it gives a qualitative conclusion about using membranes of low selectivity in separations that require high retentate purity. However, increased reliability of rigorous or molecular modeling would save a great deal of experimental work that must be done when optimizing on an empirical basis.

Although the use of low selectivity membranes may offer cost savings, the presented calculations were completed based on the assumption that the presence of the membrane step was within a hybrid process. That is, the purity of the permeate stream was not assumed to be a constraint throughout the calculations. Permeate streams containing considerable amounts of the slow permeating component would be recycled to a distillation step without disturbing the distillation operation due to its relatively small quantities. Increased amounts of the organic components in the permeate stream would decrease the mass flow of the product retentate. However, the cost calculations are based on a unit of weight of the retentate.

For stand-alone membrane processes (i.e., those not coupled to a distillation column), a 2-stage membrane process is suggested for membrane area savings. A scheme of such a process is demonstrated in Fig. 11 for ethanol dehydration. How-

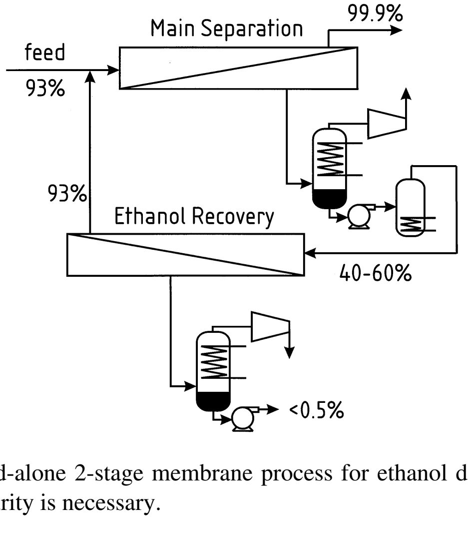

Figure 11. A stand-alone 2-stage membrane process for ethanol dehydration in which very high product purity is necessary.

Marcel Dekker, Inc.
270 Madison Avenue, New York, New York 10016

ever, it is applicable for any dehydration of organic solvents. The first stage is the dehydration stage with a low selectivity membrane. Its permeate stream of increased organic content is concentrated by a small membrane unit up to the concentration of the first feed. The second unit has a high selectivity membrane to produce high purity wastewater as permeate. This unit is relatively small because its retentate purity is lower than that of the first one so that the water content of the retentate side is sufficient to create a reasonable driving force at the end of the separation. Moreover, its feed stream is much smaller than the main feed. Simulation and optimization of this 2-stage process results in an optimum selectivity for the first membrane between 40 and 50 with an optimum permeate pressure of 8 mbar and a selectivity of 1000 for the second permeate-purification membrane with an optimum permeate pressure of 110 mbar. The cost of the second stage comprises 10.5% of the total cost of the process.

CONCLUSIONS

A method for tailoring membrane separation properties for vapor permeation within hybrid processes is presented and applied to some applications of ethanol dehydration. Membranes of a broad range of different selectivities were required, each for a specific separation range. Simulating and optimizing the whole process in an early phase offered a great deal of helpful information for determining the appropriate membrane properties required.

The results of the optimization show that the use of low selectivity membranes should be encouraged when the goal of the separation is to obtain a very pure retentate.

Running the simulations on an empirical basis requires iterative interactions with membrane development to increase the accuracy of the optimization and produce more tailored membranes for each type of application.

NOMENCLATURE

A	membrane area (m^2)
D	diffusion coefficient (m^2/s)
J_p	total permeation flux across the membrane (kg/m^2h)
$\bar{J}_P$	average total permeation flux (kg/m^2h)
L	permeability or permeation coefficient (kg/m^2hbar)
m	mass flow rate (kg/h)
p_i	partial pressure of component i
S	sorption coefficient (kg/m^3)
x	mass fraction of the most permeable component (–)

x^F	local mass fraction of the most permeable component at the feed side (–)
x^P	local mass fraction of the most permeable component at the permeate side (–)
α_L	membrane selectivity (–)
α_x	separation factor (–)
$\overline{\alpha}_x$	average separation factor (–)
δ	membrane thickness (m)
f_o	standard (reference) fugacity (bar)
θ	module cut rate (–)

Subscripts

F	feed stream
P	permeate stream
R	retentate stream
a	most permeable component
b	less permeable component
i	component i

Superscripts

F	locally on the feed side
P	locally on the permeate side

ACKNOWLEDGMENTS

Alaa Fahmy expresses his gratitude for the support provided by the Institut für Chemie of the GKSS Forschungszentrum. Dipl.-Ing. Olaf Stange is especially acknowledged for providing experimental data.

REFERENCES

1. Pressly, T.M.; Ng, K.M. A Break-even Analysis of Distillation-Membrane Hybrids. AIChE J. **1998,** *44,* 93–105.
2. Lipnizki, F.; Field, R.W.; Ten, P.K. Pervaporation-Based Hybrid Process: A Review of Process Design, Applications and Economics. J. Memb. Sci. **1999,** *153,* 183–210.
3. Stephan, W.; Noble, R.D.; Koval, C.A. Design Methodology for a Membrane/Distillation Column Hybrid Process. J. Memb. Sci. **1995,** *99,* 259–272.

4. Pettersen, T.; Argo, A.; Noble, R.D.; Koval, C.A. Design of Combined Membrane and Distillation Processes. Separ. Technol. **1996,** *6,* 175–187.
5. Moganti, S.; Noble, R.D.; Koval, C.A. Analysis of a Membrane/Distillation Column Hybrid Process. J. Memb. Sci. **1994,** *93,* 31–44.
6. Pettersen, T.; Lien, K. Design of Hybrid Distillation and Vapor Permeation Processes. J. Memb. Sci. **1995,** *102,* 21–30.
7. Rautenbach, R.; Knauf, R.; Struck, A.; Vier, J. Simulation and Design of Membrane Plants with AspenPlus. Chem. Eng. Tech. **1996,** *19,* 391–397.
8. Brüschke, H.E.A.; Schneider, W.H. Membranverfahren zur Trennung Fluider Gemische, German Patent, DE 44-10-243-C1, 1995. (in German)
9. Jansen, A.E.; Versteeg, W.F.; van Englenburg, B.; Hanemaaijer, J.H.; ter Meulen, B.P. Methods to Improve Flux During Alcohol/Water Azeotrope Separation by Vapor Permeation. J. Memb. Sci. **1992,** *68,* 229–239.
10. Will, B.; Lichtenthaler, R.N. Comparison of the Separation of Mixtures by Vapor Permeation and by Pervaporation using PVA Composite Membranes. Part 1. Binary Alcohol-Water Systems. J. Memb. Sci. **1992,** *68,* 119–125.
11. Rautenbach, R.; Meyer-Blumenroth, U. Module and Process Design for Vapor Permeation. Desalination **1990,** *77,* 295–322.
12. Helmus, F.P. Dampfpermeation: Trennvermögen, Prozessentwicklung und Einsatzmöglichkeiten, Ph.D. thesis, RWTH Aachen, 1994. (in German)
13. Sulzer Chemtech GmbH. Technical information, 1999.
14. Schehlmann, M.S.; Wiedemann, E.; Lichtenthaler, R.N. Pervaporation and Vapor Permeation at the Azeotropic Point or in the Vicinity of the LLE Boundary Phases of Organic/Aqueous Mixtures. J. Memb. Sci. **1995,** *107,* 277–282.
15. Hamada, T.; Taya, M.; Tone, S.; Nakatsuka, S. Pervaporation and Vapor Permeation Behavior of Water and 2-Propanol in Water-Selective Membranes. J. Chem. Eng. Jpn. **1997,** *30,* 600–608.
16. Okamoto, K.; Tanihara, N.; Watanabe, H.; Tanaka, K.; Kita, H.; Nakamura, A.; Kusuki, Y.; Nakagawa, K. Vapor Permeation and Pervaporation Separation of Water-Ethanol Mixtures Through Polyimide Membranes. J. Memb. Sci. **1992,** *68,* 53–63.
17. Stange, O.; Ebert, K.; Wenzlaff, A.; Wind, I.; Ohlrogge, K.; Mewes, D. The Influence of the Degree of Saturation of the Feed Vapor on the Permeability in Hybrid Processes. Proceedings of ICOM ′99, Toronto, June 1999.
18. Ebert, K.; Fritsch, D.; Stange, O.; Wenzlaff, A. Hydrophile Kompositmembran zur Entwässerung Organischer Lösungen, German Patent, Amtl. Aktenzeichen 199-25-475.3; (in press).
19. Okuno, H.; Renzo, K.; Uragami, T. Sorption and Permeation of Water and Ethanol Vapors in Poly(vinylchloride) Membrane. J. Memb. Sci. **1995,** *103,* 31–38.
20. Scharnagl, N.; Peinemann, K.V.; Wenzlaff, A.; Schwarz, H.H.; Behling, R.D. Dehydration of Organic Compounds with SYMPLEX Composite Membranes. J. Memb. Sci. **1996,** *113,* 1–5.

21. Heinz, A.; Stephan, W. A Generalized Solution-Diffusion Model of the Pervaporation Process Through Composite Membranes. Part 1. Prediction of Mixture Solubilities in the Dense Active Layer Using the UNIQUAC Model. J. Memb. Sci. **1994,** *89,* 143–151.
22. Müller-Plathe, F. Diffusion of Water in Swollen Poly(vinyl alcohol) Membranes Studied by Molecular Dynamics Simulation. J. Memb. Sci. **1998,** *141,* 147–154.
23. Hofmann, D.; Fritz, L.; Paul, D. Molecular Modeling of Pervaporation Separation of Binary Mixtures with Polymeric Membranes. J. Memb. Sci. **1998,** *144,* 145–159.
24. Hofmann, D.; Fritz, L.; Ulbrich, J.; Paul, D. Molecular Modeling of Amorphous Membrane Polymers. Polymer **1997,** *38,* 6145–6155.
25. Rautenbach, R. *Membranverfahren–Grundlagen der Modul-und Membranauslegung*; Springer: Berlin, Heidelberg, Germany, 1997. (in German)
26. Naylor, R.W.; Backer, P.O. Enrichment Calculations in Gaseous Diffusion: Large Separation Factor. AIChE J. **1955,** *1,* 95–99.
27. Collura, M.A.; Luyben, W.L. Energy-Saving Distillation Designs in Ethanol Production. Ind. Eng. Chem. Res. **1988,** *27,* 1686–1696.
28. Personal information, GKSS Forschungszentrum, Institut für Chemie, Geesthacht, Germany.
29. Huang, R.Y.M.; Rhim, J.W. Separation Characteristics of Pervaporation Membrane Separation Processes. In *Pervaporation Membrane Separation Processes*; Huang, R.Y.M., Ed.; Elsevier: Amsterdam, 1991; 111–180.
30. Rony, P.R. The Extent of Separation. In *AIChE Symposium*; New York, 1972; Ser. 120, Vol. 68, 89–104.
31. Sirkar, K.K. On the Composite Nature of the Extent of Separation. Separ. Sci. **1977,** *12,* 211–229.
32. McCandless, F.P. Stage Extent of Separation in Ideal Countercurrent Recycle Membrane Cascades. J. Memb. Sci. **1999,** *154,* 15–23.
33. Kao, Y.K.; Qiu, M.M.; Hwang, S.T. Critical Evaluation of Two Membrane Gas Permeator Designs: Continuous Membrane Column and Two Strippers in Series. Ind. Eng. Chem. Res. **1989,** *28,* 1514–1520.
34. Baudot, A.; Marin, M. Improved Recovery of an Ester Compound by Pervaporation Coupled with a Flash Condensation. Ind. Eng. Chem. Res. **1999,** *38,* 4458–4469.

Received July 2000
Revised January 2001

Downloaded At: 10:40 25 January 2011

Request Permission or Order Reprints Instantly!

Interested in copying and sharing this article? In most cases, U.S. Copyright Law requires that you get permission from the article's rightsholder before using copyrighted content.

All information and materials found in this article, including but not limited to text, trademarks, patents, logos, graphics and images (the "Materials"), are the copyrighted works and other forms of intellectual property of Marcel Dekker, Inc., or its licensors. All rights not expressly granted are reserved.

Get permission to lawfully reproduce and distribute the Materials or order reprints quickly and painlessly. Simply click on the "Request Permission/Reprints Here" link below and follow the instructions. Visit the U.S. Copyright Office for information on Fair Use limitations of U.S. copyright law. Please refer to The Association of American Publishers' (AAP) website for guidelines on Fair Use in the Classroom.

The Materials are for your personal use only and cannot be reformatted, reposted, resold or distributed by electronic means or otherwise without permission from Marcel Dekker, Inc. Marcel Dekker, Inc. grants you the limited right to display the Materials only on your personal computer or personal wireless device, and to copy and download single copies of such Materials provided that any copyright, trademark or other notice appearing on such Materials is also retained by, displayed, copied or downloaded as part of the Materials and is not removed or obscured, and provided you do not edit, modify, alter or enhance the Materials. Please refer to our Website User Agreement for more details.

Order now!

Reprints of this article can also be ordered at

http://www.dekker.com/servlet/product/DOI/101081SS100107903